

**Supplementary Information**  
**for**  
**“Synthesis and structure of the CDO zeolite precursor with a high Al**  
**content”**

Sang Hyun Ahn, Seungwan Seo, Hwajun Lee and Suk Bong Hong\*

Center for Ordered Nanoporous Materials Synthesis, Division of Environmental Science and  
Engineering, POSTECH, Pohang 37673, Korea

## Experimental Details

### Catalyst preparation and characterization

PreCDO was calcined in air at 600 °C for 8 h to be converted to a CDO zeolite (H-CDO). H-CDO was refluxed twice in 1.0 M  $\text{NH}_4\text{NO}_3$  solution (1.0 g solid per 100 mL solution) at 80 °C for 6 h. Cu-CDO was prepared by stirring  $\text{NH}_4\text{-CDO}$  three times in 0.01 M  $\text{Cu}(\text{CH}_3\text{CO}_2)_2 \cdot \text{H}_2\text{O}$  solutions at room temperature for 6 h followed by drying at 90 °C overnight and calcining at 550 °C in air for 8 h.<sup>S1</sup> For catalytic comparison, SSZ-13 (Si/Al = 16), SAPO-34 (Si/(Si + Al + P) = 0.1) and RTH (Si/Al = 10) were synthesized according to the procedures in the literature.<sup>S2</sup> Cu-SSZ-13 was prepared following the procedures similar to the Cu-CDO preparation.

Powder X-ray diffraction (XRD) patterns were recorded on a PANalytical X'pert diffractometer (Cu  $K\alpha$  radiation) with an X'Celerator detector. Elemental analysis was carried out using Jarrell-Ash Polyscan 61E inductively coupled plasma and Perkin-Elmer 5000 atomic absorption spectrometers. The  $\text{N}_2$  sorption experiments were carried out at -196 °C on a Mirae SI nanoPorosity-XG analyzer. Prior to the experiments, samples were activated under vacuum ( $10^{-3}$  torr) at 250 °C for 2 h. The temperature-programmed desorption (TPD) of  $\text{NH}_3$  was carried out on a fixed bed, flow-type apparatus linked to a Hewlett-Packard 5890 series II gas chromatograph with a thermal conductivity detector. A sample of ca. 0.1 g was activated in flowing He ( $50 \text{ mL min}^{-1}$ ) at 550 °C for 2 h. Then, 10 wt%  $\text{NH}_3$  was passed over the sample at 150 °C for 0.5 h. The treated sample was subsequently purged with He at the same temperature for 1 h to remove physisorbed  $\text{NH}_3$ . Finally, the TPD was performed in flowing He ( $30 \text{ mL min}^{-1}$ ) from 150 to 750 °C at a temperature ramp of  $10 \text{ °C min}^{-1}$ .

### Catalysis

The deNOx activity tests were conducted under atmospheric pressure in a fixed-bed flow reactor (3/8-in.-od. Al tube).<sup>S3</sup> Prior to each experiment, 0.6 g of catalyst in the 20/30 mesh size packed into the reactor were pretreated from room temperature to 500 °C at a heating rate of  $10 \text{ °C min}^{-1}$  under 21%  $\text{O}_2/\text{N}_2$  flow ( $2,000 \text{ mL min}^{-1}$ ) and kept at the final temperature for 2 h. A feed gas mixture containing 500 ppm  $\text{NH}_3$ , 500 ppm NO, 5%  $\text{O}_2$ , 10%  $\text{H}_2\text{O}$  and  $\text{N}_2$  balance was supplied through mass flow controllers, and the gas hourly space velocity (GHSV) was maintained at  $100,000 \text{ h}^{-1}$ . The inlet and outlet concentrations of NO were determined by an online Nicolet 6700 FT-IR spectrometer.

The methanol-to-olefins (MTO) conversion was conducted under atmospheric pressure in a conventional continuous-flow microreactor. Prior to the experiments, the catalyst was routinely activated under flowing  $\text{N}_2$  ( $130 \text{ mL min}^{-1}$ ) at 550 °C for 2 h and kept at 350 °C to establish a standard operating procedure, allowing time for the reactant/carrier gas distribution to stabilize. Then, methanol vapor was fed at a rate of  $0.085 \text{ mL h}^{-1}$  ( $0.67 \text{ h}^{-1}$  weight hourly space velocity (WHSV)) into the reactor containing 0.1 g of catalyst at the same temperature. The total gas flow at the reactor inlet was kept constant at  $30 \text{ mL min}^{-1}$ . The reaction products were analyzed online in a Varian CP-3800 gas chromatograph equipped with a CP-PoraPLOT Q capillary column ( $0.25 \text{ mm} \times 25 \text{ m}$ ) and a flame ionization detector, with the first analysis carried out after 5 min on stream.  $\text{CO}_2$  was separated using a packed Carbosphere column and analyzed with a thermal conductivity detector. The conversion of methanol was defined as the percentage of methanol consumed during MTO conversion. Dimethylether was not considered as a product. The yield of each product was calculated as the percentage of the amount (in mol) of methanol converted to hydrocarbons.

Ethanol (EtOH) dehydration was conducted under atmospheric pressure in a conventional continuous-flow microreactor. Prior to the experiments, each catalyst, pelletized with a diameter of 0.2-0.3 mm, was routinely activated under flowing N<sub>2</sub> (50 mL min<sup>-1</sup>) at 500 °C for 2 h and kept at the desired reaction temperature to establish a standard operating procedure, allowing time for the stabilization of reactant/carrier gas distribution. Then, ethanol vapor was fed at a rate of 0.16 mL h<sup>-1</sup> (0.64 h<sup>-1</sup> WHSV) into the reactor containing 0.2 g of the catalyst at 200 °C. The total gas flow at the reactor inlet was kept constant at 30 mL min<sup>-1</sup>. The reaction products were analyzed online in a Varian CP-3800 gas chromatograph equipped with a CP-PoraPLOT Q capillary column (0.25 mm × 25 m) and a flame ionization detector, with the first analysis carried out after 30 min on stream. The conversion of ethanol and yields of ethene and diethylether were defined as the percentages of ethanol consumed and converted to the corresponding (by)product during the reaction, respectively.

**Table S1.** Measurement conditions for multinuclear MAS NMR experiments<sup>a</sup>

	<sup>1</sup> H	<sup>13</sup> C	<sup>19</sup> F <sup>b</sup>	<sup>27</sup> Al	<sup>29</sup> Si
frequency (MHz)	500.130	125.758	376.574	130.318	99.362
pulse length (μs)	1.0	4.8	2.1	1.0	3.6
recycle delay (s)	2.0	3.0	12	2.0	30
no. of scans	100	500	64	1000	5000
reference	TMS	TMS	CFCl <sub>3</sub>	Al(H <sub>2</sub> O) <sub>6</sub> <sup>3+</sup>	TMS

<sup>a</sup> Measured on a Bruker Avance II 500 spectrometer. <sup>b</sup> Measured on a Bruker Avance II+ 400 spectrometer.

**Table S2.** Syntheses from gel composition 8.0ROH·8.0HF·1.0TMACl·8.0SiO<sub>2</sub>·1.0Al<sub>2</sub>O<sub>3</sub>·40H<sub>2</sub>O<sup>a</sup>

Run	R	Product <sup>b</sup>
1	TMA	Sodalite
2	ETMA	Ferrierite
3	DEDMA	PreCDO + sodalite
4	TEA	PreCDO
5	DMDPA	Sodalite + RUB-10
6	TPA	ZSM-5

<sup>a</sup>All the syntheses were performed under rotation (60 rpm) at 150 °C for 7 days. <sup>b</sup>The product appearing first is the major phase. TMA, tetramethylammonium; ETMA, ethyltrimethylammonium; DEDMA, diethyldimethylammonium; TEA, tetraethylammonium; DMDPA, dimethyldipropylammonium; TPA, tetrapropylammonium.

**Table S3.** Crystallographic and Rietveld refinement data for PreCDO.

Refined structure	$[(C_8H_{20}N^+)_{4.3}[(Si,Al)_{36}O_{68}(OH)_8]]$
Symmetry	Monoclinic
Space group	$P2_1/m$
$a$ (Å)	23.1128(16)
$b$ (Å)	14.1806(4)
$c$ (Å)	7.4687(5)
$\beta$ (°)	83.226(13)
Unit cell volume (Å <sup>3</sup> )	2430.8(2)
X-ray source	Beamline 9B, PAL
Geometry	Multiple analyzer system
Wavelength (Å)	1.4862
$2\theta$ scan range (°)	4.0-124.5
$2\theta$ range (°) used in refinement	4.0-100.0
No. of contributing reflections	2678
No. of geometric restraints	140
No. of refined parameters	192
$R_p$ (%)	6.5
$R_{wp}$ (%)	8.6
$R_F^2$ (%)	5.1
$\chi^2$	21.9

$$R_{wp} = [\sum w_i(Y_{io} - Y_{ic})^2 / \sum w_i Y_{io}^2]^{1/2}; R_p = \sum |Y_{io} - Y_{ic}| / \sum Y_{io}; R_F^2 = \sum |F_o^2 - F_c^2| / \sum |F_o^2|; \chi^2 = \sum w_i(Y_{io} - Y_{ic})^2 / (N_{obs} - N_{var}); D_{Wd} \text{ (Durbin-Watson statistic)} = \frac{\sum_{i=2}^N (\Delta_i / \sigma_i)}{\sum_{i=1}^N (\Delta_{i-1} / \sigma_{i-1})^2 / i}$$

**Table S4.** Atomic coordinates and thermal parameters for PreCDO.

Atom	<i>x</i>	<i>y</i>	<i>z</i>	Occup.	$U_{\text{iso}} / \times 100 \text{ \AA}^2$	Mult.
T1	0.6877(3)	0.5456(5)	0.8349(9)	1.0000	4.38(4)	4
T2	0.8866(3)	0.5473(5)	-0.0315(9)	1.0000	4.38(4)	4
T3	0.8105(3)	0.0492(5)	0.6999(10)	1.0000	4.38(4)	4
T4	0.8089(3)	0.4516(5)	0.2799(10)	1.0000	4.38(4)	4
T5	0.6129(3)	0.4473(5)	0.5749(10)	1.0000	4.38(4)	4
T6	0.6836(3)	0.9538(5)	0.2499(10)	1.0000	4.38(4)	4
T7	0.7380(4)	0.75	0.7281(11)	1.0000	4.38(4)	2
T8	0.8273(4)	0.75	-0.0033(11)	1.0000	4.38(4)	2
T9	0.7185(4)	0.75	0.3190(11)	1.0000	4.38(4)	2
T10	0.7547(4)	0.25	0.1979(11)	1.0000	4.38(4)	2
T11	0.6753(4)	0.25	0.5401(11)	1.0000	4.38(4)	2
T12	0.7789(4)	0.25	0.7869(11)	1.0000	4.38(4)	2
O1	0.8201(3)	0.1575(3)	0.7604(12)	1.0000	5.42(9)	4
O2	0.8556(3)	0.5150(5)	0.7964(7)	1.0000	5.42(9)	4
O3	0.6673(4)	0.5310(6)	0.0469(6)	1.0000	5.42(9)	4
O4	0.74406(21)	0.4825(5)	0.7675(12)	1.0000	5.42(9)	4
O5	0.8675(3)	0.6571(3)	0.0137(12)	1.0000	5.42(9)	4
O6	0.9564(3)	0.5391(9)	-0.0756(17)	1.0000	5.42(9)	4
O7	0.7024(3)	0.657(3)	0.8013(12)	1.0000	5.42(9)	4
O8	0.63347(23)	0.5176(5)	0.7268(7)	1.0000	5.42(9)	4
O9	0.6787(3)	0.8426(3)	0.3022(12)	1.0000	5.42(9)	4
O10	0.6385(3)	0.4855(5)	0.3796(7)	1.0000	5.42(9)	4
O11	0.8240(4)	0.4614(7)	0.4850(6)	1.0000	5.42(9)	4
O12	0.75086(20)	0.5139(5)	0.2571(13)	1.0000	5.42(9)	4
O13	0.6375(3)	0.3427 (3)	0.6022(12)	1.0000	5.42(9)	4
O14	0.542(3)	0.4465(9)	0.5965(18)	1.0000	5.42(9)	4
O15	0.7923(3)	0.3423(3)	0.2416(12)	1.0000	5.42(9)	4
O16	0.8636(3)	0.4837(5)	0.1422(7)	1.0000	5.42(9)	4
O17	0.7457(4)	0.75	0.5104(6)	1.0000	5.42(9)	2
O18	0.773(3)	0.75	0.1571(8)	1.0000	5.42(9)	2
O19	0.8014(3)	0.75	0.8036(8)	1.0000	5.42(9)	2
O20	0.7437(4)	0.25	-0.0128(7)	1.0000	5.42(9)	2
O21	0.7351(3)	0.25	0.6348(8)	1.0000	5.42(9)	2
O22	0.6926(3)	0.25	0.3230(8)	1.0000	5.42(9)	2
N1	0.99476(10)	0.18718(11)	0.55947(23)	0.517(3)	1.00(3)	4
C2	0.96786(11)	0.23587(20)	0.4059(3)	0.517(3)	1.00(3)	4
C3	0.92386(13)	0.1733(3)	0.3190(6)	0.517(3)	1.00(3)	4
C4	0.99426(10)	0.2346(3)	0.7432(3)	0.517(3)	1.00(3)	4
C5	0.93106(10)	0.2222(13)	0.8314(9)	0.517(3)	1.00(3)	4
C6	1.00985(20)	0.08457(12)	0.5105(6)	0.517(3)	1.00(3)	4
C7	1.03421(22)	-0.00465(18)	0.5963(6)	0.517(3)	1.00(3)	4
C8	1.04588(8)	0.25637(23)	0.5363(6)	0.517(3)	1.00(3)	4
C9	1.10455(10)	0.2456(15)	0.6076(6)	0.517(3)	1.00(3)	4

N10	0.47491(7)	0.65909(17)	0.94832(22)	0.547(4)	1.00(3)	4
C11	0.51325(9)	0.6766(7)	1.0933(3)	0.547(4)	1.00(3)	4
C12	0.56657(13)	0.6918(10)	0.9543(5)	0.547(4)	1.00(3)	4
C13	0.43132(13)	0.58081(12)	0.9211(12)	0.547(4)	1.00(3)	4
C14	0.4238(7)	0.47608(15)	0.902(3)	0.547(4)	1.00(3)	4
C15	0.41778(8)	0.71210(22)	1.0068(4)	0.547(4)	1.00(3)	4
C16	0.37410(13)	0.663(3)	0.8951(5)	0.547(4)	1.00(3)	4
C17	0.49957(18)	0.65877(21)	0.7506(3)	0.547(4)	1.00(3)	4
C18	0.53400(20)	0.73797(21)	0.6420(6)	0.547(4)	1.00(3)	4

---



**Table S5.** Selected bond lengths and angles for PreCDO.

Bond length / Å		Bond angle / °	
T1-O3	1.611(8)	O3-T1-O4	111.5(6)
T1-O4	1.612(9)	O3-T1-O7	107.9(6)
T1-O7	1.629(8)	O3-T1-O8	107.8(5)
T1-O8	1.618(9)	O4-T1-O7	110.1(5)
T2-O2	1.611(9)	O4-T1-O8	110.7(5)
T2-O5	1.643(8)	O7-T1-O8	108.7(6)
T2-O6	1.611(9)	O2-T2-O5	107.4(6)
T2-O16	1.617(9)	O2-T2-O6	110.2(6)
T3-O1	1.624(9)	O2-T2-O16	110.3(5)
T3-O2	1.615(10)	O5-T2-O6	110.4(6)
T3-O4	1.622(9)	O5-T2-O16	107.9(5)
T3-O11	1.605(8)	O6-T2-O16	110.5(7)
T4-O11	1.617(9)	O1-T3-O2	107.0(6)
T4-O12	1.630(10)	O1-T3-O4	109.3(6)
T4-O15	1.630(9)	O1-T3-O11	110.5(6)
T4-O16	1.599(9)	O2-T3-O4	109.9(5)
T5-O8	1.623(10)	O2-T3-O11	109.5(6)
T5-O10	1.602(9)	O4-T3-O11	110.5(6)
T5-O13	1.611(9)	O11-T4-O12	108.9(6)
T5-O14	1.629(9)	O11-T4-O15	109.2(6)
T6-O3	1.619(9)	O11-T4-O16	110.0(6)
T6-O9	1.626(9)	O12-T4-O15	106.5(6)
T6-O10	1.592(10)	O12-T4-O16	112.1(6)
T6-O12	1.628(9)	O15-T4-O16	110.0(6)
T7-O7	1.616(7)	O8-T5-O10	108.8(5)
T7-O17	1.614(9)	O8-T5-O13	109.9(6)
T7-O19	1.630(11)	O8-T5-O14	108.1(6)
T8-O5	1.625(8)	O10-T5-O13	109.2(6)
T8-O18	1.630(10)	O10-T5-O14	110.6(7)
T8-O19	1.626(11)	O13-T5-O14	110.3(6)
T9-O9	1.617(8)	O3-T6-O9	109.7(6)
T9-O17	1.628(11)	O3-T6-O10	106.8(6)
T9-O18	1.639(10)	O3-T6-O12	108.8(6)
T10-O15	1.625(8)	O9-T6-O10	110.8(5)
T10-O20	1.623(10)	O9-T6-O12	107.8(6)
T10-O22	1.620(11)	O10-T6-O12	112.8(6)
T11-O13	1.615(7)	O7-T7-O7	109.4(7)
T11-O21	1.626(11)	O7-T7-O17	109.4(5)
T11-O22	1.623(10)	O7-T7-O19	109.0(5)
T12-O1	1.620(8)	O7-T7-O17	109.4(5)
T12-O20	1.616(10)	O7-T7-O19	109.0(5)
T12-O21	1.608(11)	O17-T7-O19	110.6(6)
T-O (Avg.)	1.620	O5-T8-O5	108.3(7)
N1-C2	1.532(3)	O5-T8-O18	109.9(5)
N1-C4	1.526(3)	O5-T8-O19	110.1(5)

N1-C6	1.531(3)	O5-T8-O18	109.9(5)
N1-C8	1.53(3)	O5-T8-O19	110.1(5)
N10-C11	1.499(3)	O18-T8-O19	108.6(6)
N10-C13	1.529(4)	O9-T9-O9	108.5(7)
N10-C15	1.538(3)	O9-T9-O17	110.5(5)
N10-C17	1.52(3)	O9-T9-O18	109.8(4)
C2-C3	1.549(4)	O9-T9-O17	110.5(5)
C4-C5	1.540(4)	O9-T9-O18	109.8(4)
C6-C7	1.553(5)	O17-T9-O18	107.8(7)
C8-C9	1.522(4)	O15-T10-O15	107.4(7)
C11-C12	1.530(4)	O15-T10-O20	110.1(5)
C13-C14	1.504(4)	O15-T10-O22	110.0(4)
C15-C16	1.549(5)	O15-T10-O20	110.1(5)
C17-C18	1.549(5)	O15-T10-O22	110.0(4)
		O20-T10-O22	109.2(7)
		O13-T11-O13	108.9(7)
		O13-T11-O21	109.5(5)
		O13-T11-O22	110.4(5)
		O13-T11-O21	109.5(5)
		O13-T11-O22	110.4(5)
		O21-T11-O22	108.3(6)
		O1-T12-O1	108.2(7)
		O1-T12-O20	109.7(5)
		O1-T12-O21	108.9(5)
		O1-T12-O20	109.7(5)
		O1-T12-O21	108.9(5)
		O20-T12-O21	111.4(7)
		O-T-O (Avg.)	109.5

---

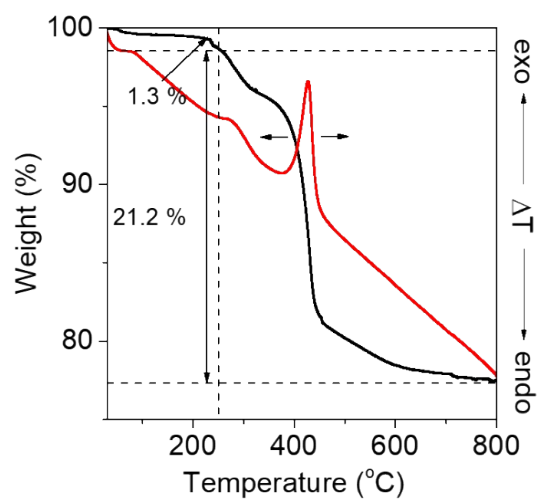


**Fig. S1** TGA/DTA curves of PreCDO.

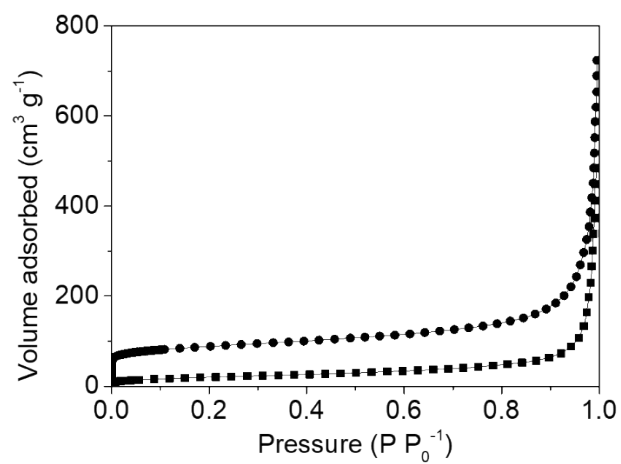


**Fig. S2** N<sub>2</sub> adsorption isotherms on PreCDO (■) and its calcined form (●).

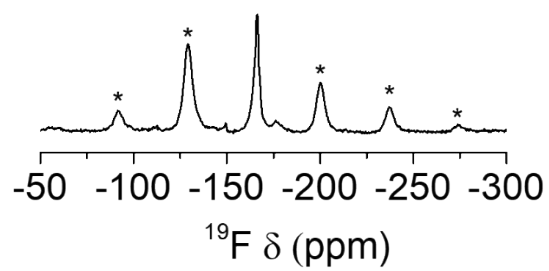


**Fig. S3**  $^{19}\text{F}$  MAS NMR spectrum of as-made PreCDO. Spinning side bands are marked by asterisks.

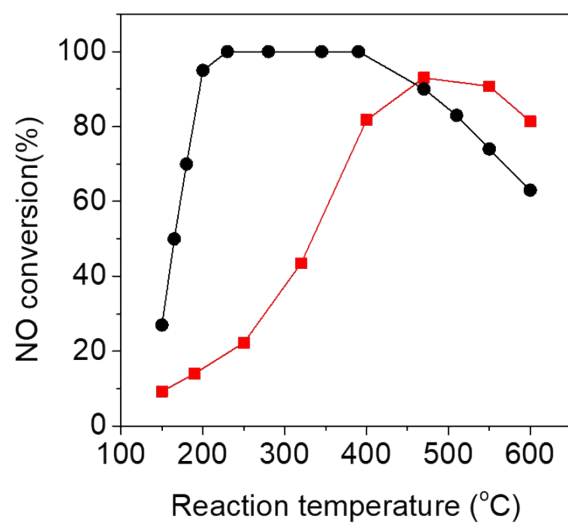


**Fig. S4** NO conversion as a function of temperature in  $\text{NH}_3$ -SCR reaction over Cu-CDO (■) and Cu-SSZ-13 (●). The feed contains 500 ppm of  $\text{NH}_3$ , 500 ppm of NO, 5%  $\text{O}_2$ , 10%  $\text{H}_2\text{O}$  balanced with  $\text{N}_2$  at  $100,000 \text{ h}^{-1}$  GHSV.

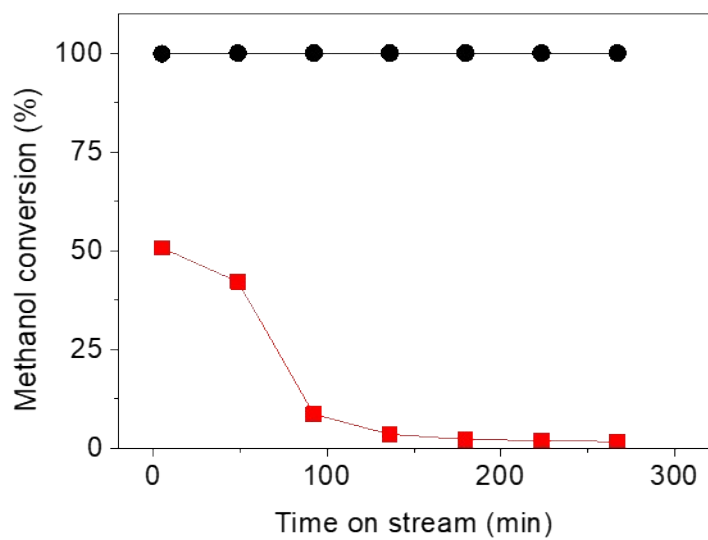


**Fig. S5** Methanol conversion as a function of time on stream in the MTO reaction over H-CDO (■) and H-SAPO-34 (●) at 350 °C and 0.67 h<sup>-1</sup> WHSV.

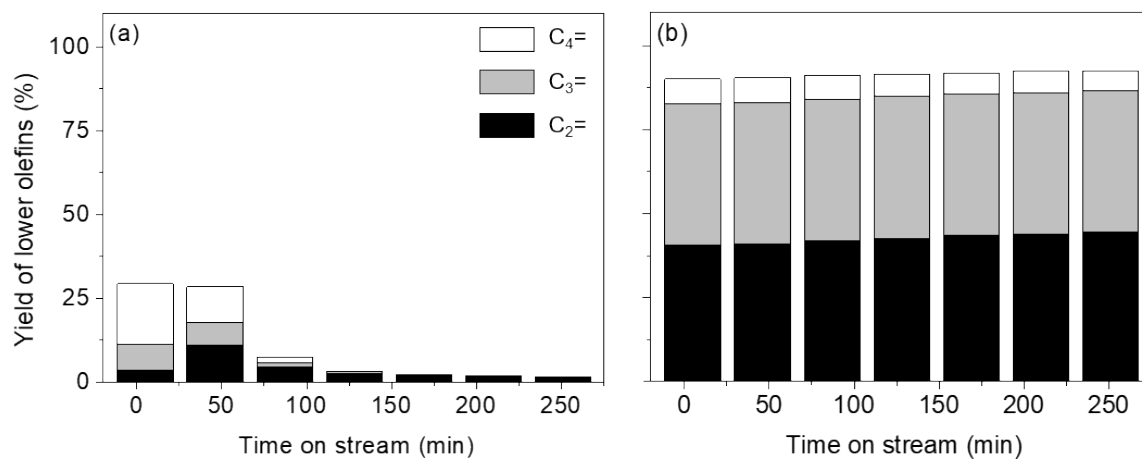


**Fig. S6** Yield of lower olefins as a function of time on stream in the MTO reaction over (a) H-CDO and (b) H-SAPO-34 at 350 °C and 0.67 h<sup>-1</sup> WHSV.



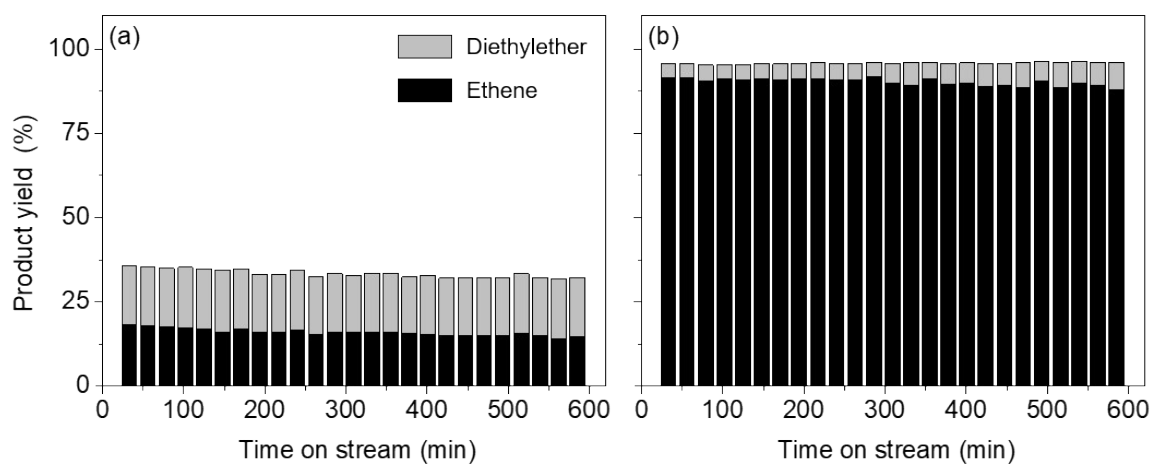


**Fig. S7** Yield of ethane and diethylether as a function of time on stream in the ethanol dehydration over (a) H-CDO and (b) H-RTH at 200 °C and 0.64 h<sup>-1</sup> WHSV.

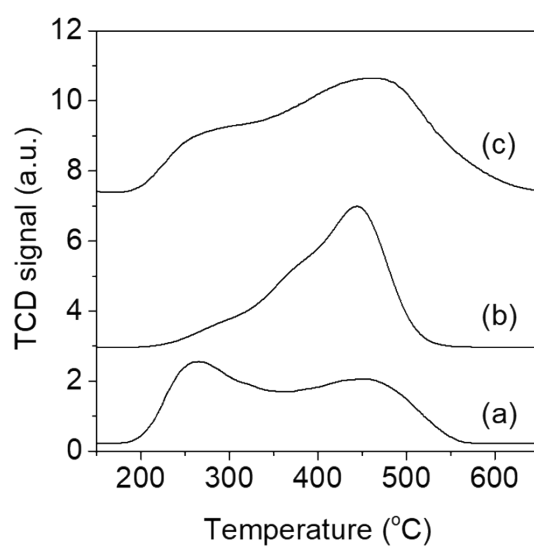


**Fig. S8** NH<sub>3</sub> TPD profiles from (a) H-CDO, (b) H-SAPO-34 and (c) H-RTH.

**References**

- S1 I. J. Heo, Y. M. Lee, I.-S. Nam, J. W. Choung, J.-H. Lee and H.-J. Kim, *Microporous Mesoporous Mater.*, 2011, **141**, 8-15.
- S2 (a) S. I. Zones, US Pat., 4,544,538, 1985; (b) S. I. Zones, *J. Chem. Soc., Faraday Trans.*, 1991, **87**, 3709-3716; (c) H. G. Jang, H.-K. Min, J. K. Lee, S. B. Hong and G. Seo, *Appl. Catal., A*, 2012, **437**, 120-130; (d) D. Jo, J. B. Lim, T. Ryu, I.-S. Nam, M. A. Cambor and S. B. Hong, *J. Mater. Chem. A* **2015**, *3*, 19322-19329.
- S3 J. H. Park, H. J. Park, H. J. Baik, I.-S. Nam, C. H. Shin, J.-H. Lee, B. K. Cho and S. H. Oh, *J. Catal.*, 2006, **240**, 47-57.